Land-Use/-Cover Dynamic Modeling Using RS and GIS with Emphasis on Maximum Likelihood Rule and Transition Matrix

Tarbiat Modares University

Author
Banafshe Yasrebi, *Ph.D.*[1*]
Hamid Reza Abbasi, *Ph.D.*[2]
Koroush Behnamfar, *Ph.D.*[3]
Mehri Dinarvand, *Ph.D.*[4]

[1]Ph.D., Forests and Rangelands Research Department, Khuzestan Agricultural and Natural Resources Research and Education Center, AREEO, Ahvaz, Iran.
[2]Ph.D., Desert Department of Institute of Forests and Rangelands, Agricultural Research, Education and Extension Organization (AREEO), Tehran, Iran.
[3]Ph.D., Forests and Rangelands Research Department, Khuzestan Agricultural and Natural Resources Research and Education Center (AREEO), Ahvaz, Iran.
[4]Ph.D., Forests and Rangelands Research Department, Khuzestan Agricultural and Natural Resources Research and Education Center (AREEO), Ahvaz, Iran.

* Correspondence
Address: Forests and Rangelands Research Department, Khuzestan Agricultural and Natural Resources Research and Education Center, AREEO, Ahvaz, Iran.
Tel: (+98) 6133737373
Fax: (+98) 6133737400
P.O. Box: 61335-3341, Ahvaz,
Email: b.yasrebi@areeo.ac.ir

A B S T R A C T

Aims: Understanding the land-use and land-cover (LULC) change pattern is important for prospering environmental restoration. The present study aimed to study changes in LULC patterns of the Koupal Watershed in Khuzestan Province.

Materials & Methods: This study focused on changes in LULC patterns using remote sensing techniques and geographic information systems (GIS). For this purpose, the Multi-temporal satellite images of the Landsat series (1998 and 2020) were acquired, preprocessed, and used to extract LULC maps by machine learning method including the Bayes discriminant and Maximum likelihood rule over 22 years. The reliability of classified maps was checked using a confusion matrix. The transition matrix and change rate were extracted by change detection analysis.

Findings: Change detection analysis shows that vegetation cover witnessed of dramatic decrease and changed from 27.6% to 0.06%, followed by water body reduction from 8.59% to 0.79% and bare land decrease from 57.9% to 51% of the whole area and a rapid expansion of cropland from 5.44% to 41.25%. The change matrix revealed that 93% of cropland remained unchanged, followed by bare land (71%), built-up (53%), water body (7%), sand dune (6%), and vegetation (0.05%).

Conclusion: These results establish LULC trends in the past 22 years and provide useful data for planning and sustainable land-use management. The findings presented in the study should be applied as an approach to create awareness and increase land-cover protection and halt land-cover change.

CITATION LINKS

[1] Halimi M., Sedighifar Z., Mohammadi C. Analyzing ... [2] Twisa S., Buchroithner M. F. Land-use and ... [3] Gifawesen S. T. Review on effects of land use ... [4] Mansour S., Al-Belushi M., Al-Awadhi T. Monitoring land use ... [5] Koko A. F., Yue W., Abubakar G. A., Hamed R., Alabsi A. A. Monitoring and ... [6] Naikoo M. W., Rihan M., Ishtiaque M., Shahfahad N. Analyses of ... [7] Swain J. B., Patra K. C. Impact assessment of land use/land cover ... [8] Traore M., Lee M. S., Rasul A., Balew A. Assessment of land ... [9] Kamali Maskooni E., Hashemi H., Berndtsson R., Daneshkar Arasteh P., Kazemi M. Impact of ... [10] Popov M., Michaelides S., Stankevich S., Kozlova A., Piestova I., Lubskiy M. Assessing... [11] Chughtai A. H., Abbasi H., Karas I. R. A review on ... [12] Si Salah H., Goldin S. E., Rezgui A., Nour El Islam B., Ait-Aoudia S. What is a ... [13] Feranec J., Hazeu G., Christensen S., Jaffrain G. Corine land ... [14] Negassa M. D., Mallie D. T., Gemeda D. O. Forest cover change... [15] Os B., Aa A. Change detection in ... [16] Sam Navin M., Agilandeeswari L. Comprehensive ... [17] Hamidi M. Atmospheric investigation of frontal dust storms in southwest Asia. Asia-Pac. J. Atmos. Sci. 2018; 55(2): 177-193 ... [18] Campbell J. B., Wynne R. H. Introduction ... [19] Anonymous. Fundamentals ... [20] Richards J. S. Remote sensing digital image analysis. Springer, 2013. 502 p ... [21] Jenson J. R. Introductory digital ... [22] Ikiel C., Dutucu A. A., Ustaoglu B., Kilic D. E. Land use... [23] Tilahun A. Accuracy assessment of land use land cover classification ... [24] Congalton R. G. Accuracy assessment and validation of ... [25] Janssen L.L.F., van der Wel F.J.M. Accuracy assessment... [26] Fung T., LeDrew E. The determination of ... [27] Congalton R. G., Oderwald R. G., Mead R. A. Assessing Landsat classification accuracy using discrete multivariate analysis statistical techniques. Photogramm. Eng. Remote Sens.1983;9(12):1671-1678 ... [28] Lotfi Nasab S., Dargahian F., Khosrowshahi M. Water quality assessment of... [29] Moradi F., Kaboli H. S., Lashkarara B. Projection of future land use/cover change in the Izeh-Pyon Plain ... [30] Gheitury M., Heshmati M., Ahmadi M. Longterm land use change detection in Mahidasht ... [31] Khoshnood Motlagh S., Sadoddin A., Haghnegahdar A., Razavi S., Salmanmahiny A., Ghorbani K. Analysis and prediction of land cover changes using the land change modeler (lcm) in a semiarid ...

Introduction

One of the major problems facing worldwide today is how to protect Ecosystems. Land degradation due to land-use and land-cover change (LULC), causes important environmental and social problems. Land-cover is the physical characteristics of landscape including vegetation, water, soil, and those created by human activities for example towns while land-use is the way that land has been used by humans [1].

Watersheds are dynamic systems by nature; therefore, they change constantly. The rapid changes of LULC, particularly in developing countries, cause the reduction of fundamental resources e.g., water, soil, vegetation, and saline lands expansion [2] biodiversity loss [3]. Destruction and loss of fertile lands and natural habitats occur as a result of unplanned urban expansion [4-6], cropland expansion [2], soil erosion, surface runoff [8], desertification, urban heat island [9], climate change [11], deforestation and mining [12]. Change detection is defined as the process of identifying differences in the state of an object or phenomenon by observing it at different times [13]. This is an active research area with a broad range of applications from simple differencing to machine learning techniques [14].

LULC change detection at a local scale is an important tool to monitor the sustainability of ecological systems supporting human needs [7] and show the processes caused either by anthropogenic or natural factors [15] by understanding the characteristics, extent, and pattern of land-use/-cover change is an important supporting tool for decision making processes and quantitative assessment of LULC change dynamics to manage and understand the landscape transformation [16] at different spatial as well as temporal scales. Hence, LULC studies can help solve environmental problems.

Recently, remote sensing and GIS has been proven to be a very useful tool in analyzing LULC change. The rapid development of earth observation technology provides courtesy, long-term in different resolution satellite imagery resources for research. Various studies have effectively mapped and analyzed LULC changes using data obtained from different sensors [18].

The Koupal Watershed is located in southwestern Iran in Khuzestan Province with an arid climate. Passing through the city of Ahvaz and moving south around, only deserts and saline land with low vegetation cover and rainfed cropland can be seen.

The dust storm on February 18, 2017, damaged electrical infrastructure and power failure in Khuzestan Province, according to NASA's natural hazard list [19]. Following then, the topic of desertification in Khuzestan was raised. Droughts and climate change are frequently mentioned as key elements in desertification in official speeches. Old photographs indicate Sharifa wetland in the investigated region, but these days no sign of it, and the sabkha (saline land) has replaced the wetland with the top priority of stabilization, and a land moisturizing project to avoid dust emission is ongoing. LULC change results in rapid desertification, particularly in arid and semi-arid areas, and is often ignored as a key desertification factor.

Many studies have studied LULC change using RS images, however, very few studies have focused on quantifying positive and negative change rates. Indeed, the novelty of this study is the quantification of the LULC change rate in an arid region that has led to desertification. It can be used as a tool for better management, planning, and policy-making for an ecologically fragile region. Hence, this research quantified the pattern of LULC change by maximum likelihood classifier algorithm and justified that LULC change can have a dramatic role in desertification.
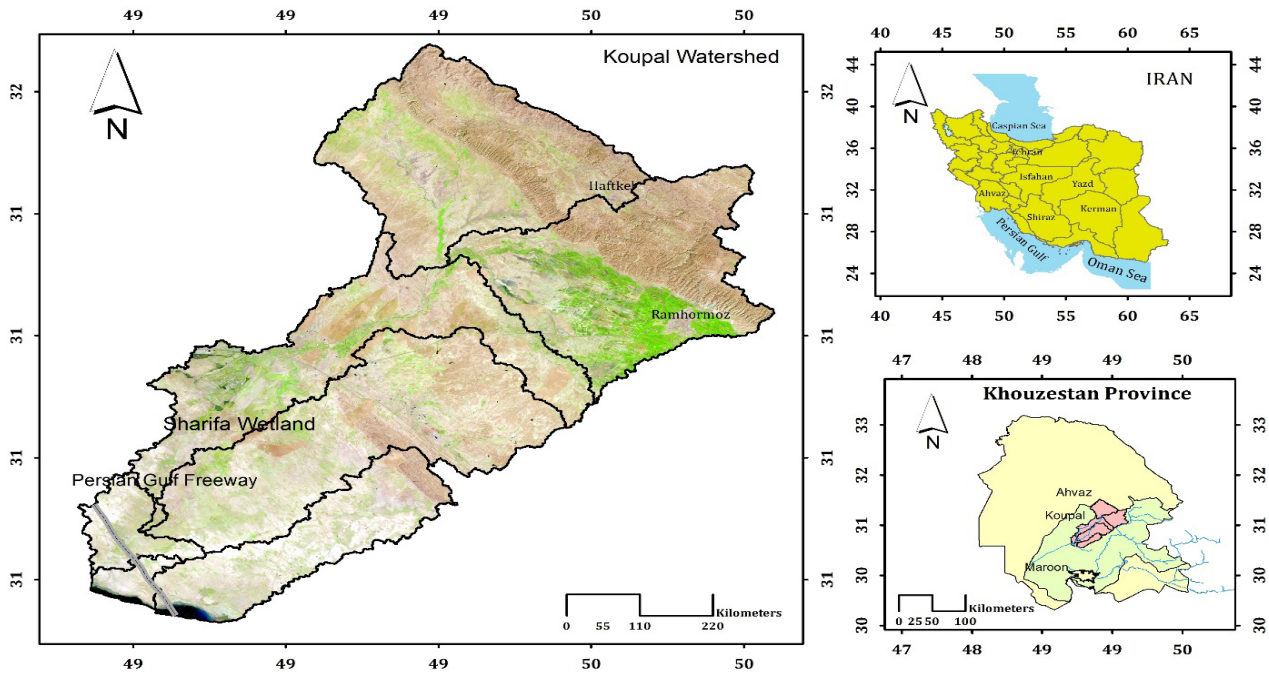
Figure 1) Location map of the study area.

Materials & Methods
Study area
The study area is located in 30.91 to 31.48 latitude and 49.25 to 49.35 longitude with an area of 290000 ha in the southeast of Ahvaz City in Khuzestan Province, it is one of the sub-basins of the Maroon-Jarahi River and a part of the Persian Gulf large basin, as depicted in Figure 1. The river originates in the north of Ramhormoz city and forms the Ramhormoz alluvial fan by passing through the mountains and finally forming Sharifa wetland in the southeastern plains around Ahvaz [20].

The Koupal Watershed is morphologically divided into three main units: mountain, plain, and playa. The mountainous part is formed from Gachsaran Formation with facies of irregular slopes covered by sparse *Ziziphus spina-christi* trees and trapped sand dunes. The plain unit is an alluvial fan that is almost entirely covered by croplands. Ahvaz, Maroon, and Koupal faults formed a tectonic playa unit filled with Quaternary sediment [21]. Due to the change in elevation from 660m in the northern part to 8 m in the southern part

of the watershed, annual rainfall varies from 350 mm to 200 mm from north to south. The maximum temperature ranges from 24 to 33 degrees Celsius, while the lowest temperature ranges from 5 to 18 degrees Celsius, with an average temperature of 24 degrees Celsius. The climate of the research area varies from semi-arid mild to temperate desert, based on the Emberger climate classification. Natural vegetation zones are changed from semi-steppe to warm steppe, due to the changing conditions, a wide range of plants can be seen, from the *Ziziphus nummularia* and *Ziziphus spina christi* in the mountainous part to halophytes species in the southern part of the study area [23].

Satellite Data Preparation
In this study, LULC change dynamics were utilized by two remotely sensed satellite images at an interval of 22 years. These images comprised Landsat TM (5) for 1998, and Landsat OLI (8) for 2020. The Landsat image scenes were acquired from the freely accessible data portal (http://earthexplorer.usgs.gov/) of the United States Geological Survey (USGS). The downloaded images

Table 1) Satellite images used in the study.

No.	Satellite Name	Acquisition Date	WRS Path/ Row	Sensor Type	LULC Name	UTM Zone	Spatial Resolution(m)
1	Landsat 5	1998.03.06	165/38	TM	98LULC	39	30×30
2	Landsat 8	2020.03.02	165/38	OLI	2020LULC	39	30×30
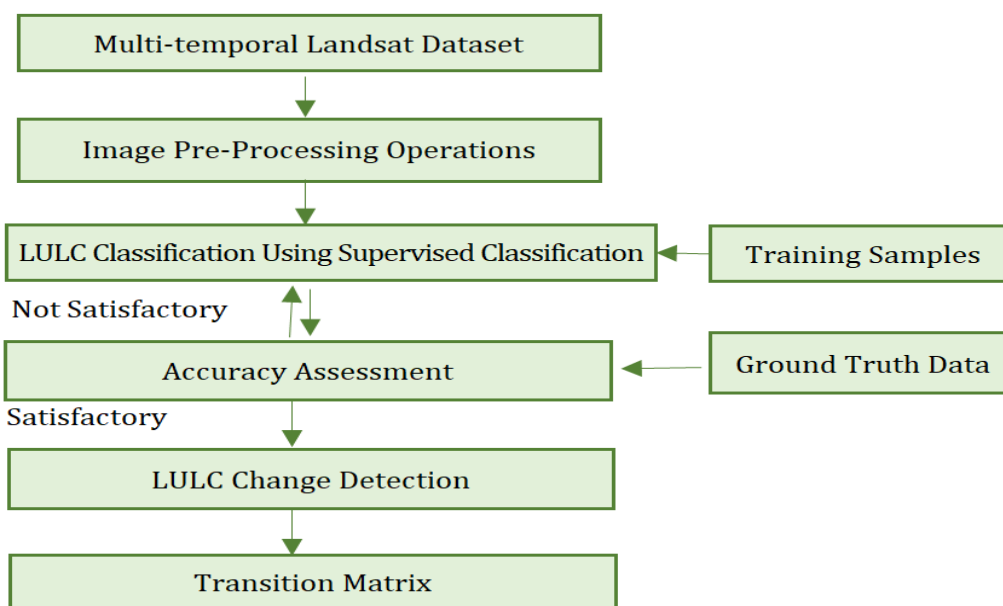
Figure 2) Research methodological flowchart.

were already geo-referenced and projected to the Universal Transverse Mercator (UTM) map zone 39 N, with a datum and ellipsoid of WGS84. The various pre-processing operations were conducted in ENVI 5.3 and ArcGIS 10.3.1 image processing soft wares. Table 1 present the different Landsat datasets used in the study.

Field Data Collection

A random field survey of the different parts of the studied watershed had been conducted to identify the LULC classes. The identified land-cover classes were matched with similar types observed in the satellite images to interpret the different spectral signatures of the LULC class on each image. The prominent land-cover types identified in both the satellite images and a field survey conducted included built-up areas, bare lands, vegetation cover, water bodies, croplands, and trapped sand dunes. These observations were utilized to classify and map the 6-broad land-cover types in the 1998 LULC map and 7 land-cover classes for the 2020 LULC map owing to afforestation area were added.

The methodological approach employed in this study was subdivided into 4 stages. These stages are as follows: (i) pre-processing of satellite data, (ii) image classification, (iii) accuracy assessment, and (iv) LULC change detection. Figure 2 illustrates the flowchart of the methodology.

Image pre-processing

Pre-processing is an essential technique used to improve the quality of raw satellite data. The satellite data can be calibrated by using the process of atmospheric and radiometric

Table 2) Land-use/land-cover (LULC) classification Description.

No	Land-Use/Land-Cover Types	Description
1	Built-up/urban areas	Areas that include residential, industrial, and commercial areas, mixed-use buildings, roads, and other transport facilities.
2	Vegetation	Areas that include scrub and grasslands
3	Bare lands	Includes areas with exposed soils, un-vegetated lands
4	Water bodies	Includes rivers, streams, lakes, ponds, and various reservoirs.
5	Sand dunes	Areas with wind erosion facies include trapped sand dunes, Barkhans
6	Croplands	It comprises agricultural and fallow lands
7	Afforestation	It Includes an area with a tree plantation

corrections. Radiometric correction helps to correct digital number errors and atmospheric correction helps to correct the atmospheric effects on the reflectance values of the satellite images than for land sat 8 images to increase the resolution to 8 meters by Panchromatic band fusion to multispectral band followed by rescaling. Eventually mosaicking the Landsat scenes and resulting images were clipped to the study area.

Image classification

Land-use and cover maps can be prepared by image classification methods and divided into two categories: Unsupervised methods (e.g., ISODATA, K-means) are based on automated computational frameworks that typically produce binary maps and indicate whether a change has occurred. The analyst applies homogeneous samples in different land-cover classes as training areas samples in supervised classification (e.g., Maximum likelihood method, SVM, Random forest) [25]. The pixels in the satellite images are trained and separated into LULC classes through the learning process. In this study, the Bayes discriminant function shown in the first equation and the Maximum likelihood rule was used to classify the acquired satellite images.

$$gi(x) = lnp(wi) - \frac{1}{2}ln|\sum i| - \frac{1}{2}(x - mi)^T \sum_i^{-1}(X - mi)$$

Eq. (1)

where i class, x n-dimensional data (where n is the number of bands), p(wi) probability that class wi occurs in the image and is assumed the same for all classes, |Σi| determinant of the covariance matrix of the data in class wi, Σi-1 its inverse matrix, mi mean vector [26].

The maximum likelihood is one of the most widely used algorithms due to its availability and simple training process, probability-based [13, 27]. In this decision rule, the probability of a pixel belonging to each of a predefined set of classes is calculated, and then the pixel is assigned to the class for which the probability is the highest [24]. The input bands used in the study to produce false-color composite maps consisted of bands 4, 3, and 2, for Landsat TM and bands 5, 4, and 3, for Landsat 8 OLI.

The spectral signature of each image pixel was matched with the training samples of the study area and the satellite images were classified into built-up/urban area, vegetation, bare land, and water bodies, sand dunes and croplands, and afforestation were added in 2020 land-cover map as described in Table 2. In image classification, 156541 pixels for land sat TM and 294310 pixels for land sat OLI were used as training samples using the region of interest (ROI) tool in ENVI 5.3 image processing software.

Quantitative Accuracy Assessment

An important stage in classification methods is reliability and accuracy evaluation of results.

Table 3) Assessment of classification accuracy.

| LULC Classes	1998		2020	
	Producer's Accuracy	User's Accuracy	Producer's Accuracy	User's Accuracy
Vegetation	75.41	88.00	100	100
Waterbody	89.92	83.27	100	100
Sand Dune	78.14	100	100	100
Bare Land	99.96	94.19	72.22	76.47
Cropland	90.33	90.1	87.5	75
Build Up	73.25	100	100	100
Afforestation	-	-	78.57	100
Overall Accuracy	93.10		88.42	
Kappa	0.85		0.86	

After collecting ground reference test data from random samples, the pixel or polygon base test data are compared with the remote sensing-derived classification map. [27]. The two broad methods of assessing a classified image's accuracy are the confusion (error) matrix technique and the receiver operating characteristic (ROC) curve. An error matrix is the most common way to present the accuracy of the classification results [28] an error matrix or confusion matrix is organized in rows and columns which express the number of sample units allocated to a specific category relative to the actual category as indicated by the reference data. The columns usually represent the reference data while the rows indicate the classification generated from the remotely sensed data. Google Earth is a powerful and attractive source of positional data that can be used for reference data with suitable accuracy and low cost [29]. Dividing the total correct samples by the total number of samples is called 'overall accuracy' and the total number of correct samples in a class is divided by the total number of samples of that class as derived from the reference data indicates the probability of a reference

sample is correctly classified and is omission error or called 'producer's accuracy' because the producer of the classification is interested in how well a certain area can be classified if a total number of correct samples in each class is divided by the total number of samples is commission error called often user's accuracy or reliability, indicates of the probability that a sample classified on the image represents that category on the ground [30].

Another approach is to calculate the Kappa-coefficient, which is a discrete multivariate technique of use in accuracy assessment. It is a measure of accuracy between the remote sensing derived classification map and reference data that ranges into three groupings: a value greater than 0.80 (i.e. 80%) represents strong agreement; a value between 0.40 and 0.80 (i.e. 40– 80%) represents a moderate agreement, and a value below 0.40 (i.e. 40%) represents poor agreement [30].

Change Detection

Change detection involves the use of multi-temporal datasets to discriminate areas of land-cover change between dates of imaging so to perform land-cover change
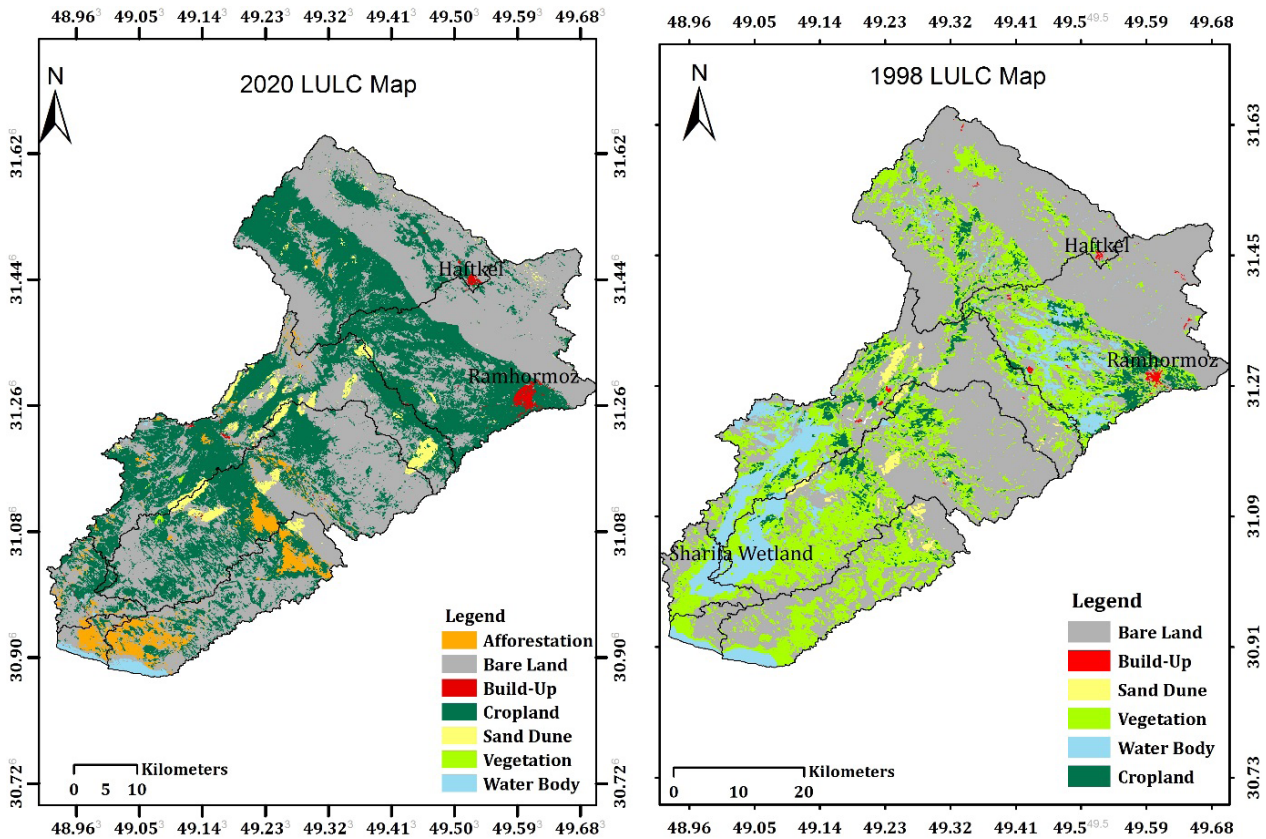
Figure 3) Classified LULC of the Koupal Watershed in 1998 and 2020.

analysis, change detection workflow in remote sensing software was applied [5, 6, 16]. The change matrix showed the overall quantitative LULC changes and the gains and losses in each land-cover type from 1998 to 2020 then followed by the statistical and graphical analysis of LULC losses and gains in each class by GIS techniques in ARC Map 10.3 and Excel.

Findings

Accuracy assessment

The overall accuracy of the classification image (error matrix analysis) results for 1998 shows an overall accuracy of 93.1% (39790 from 42738 randomly selected test points were correctly classified) with a Kappa coefficient of 0.85, in 2020LULC map shows an overall accuracy of 88.42% (7308 from 8265 randomly selected test points were correctly classified. The values of kappa coefficients for both LULC maps were

found to be above 80% as shown in Table 3. This indicates a reliable and accurate classification of images for analyzing LULC change.
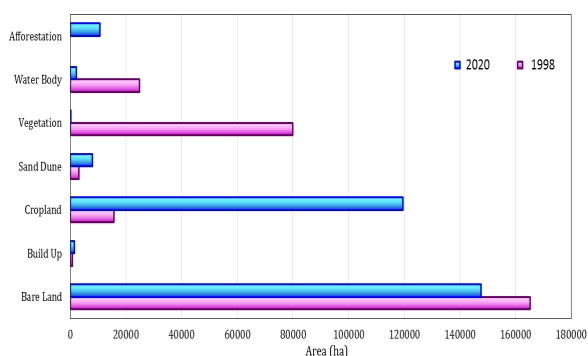
Land-Use/ Land-Cover Change Detection

It was observed the land-use and land-cover pattern in the studied area has changed dramatically between 1998 and 2020, with cropland growth over the last two decades. Figure 3 displays the spatial distribution of both LULC in 1998 and 2020 and quantitative statistics are presented in Table 4.

LULC pattern comparison in two classification maps indicates watershed's vegetation cover witnessed of dramatic decrease and changed from 27.6% to 0.06%, followed by water body reduction from 8.59% to 0.79% and bare land decrease from 57.9% to 51% of the whole area. The results indicate a rapid expansion of cropland from 5.44% to 41.25% of the total area. Sand dunes increased from 1.08% of

Table 4) Land-use/ land-cover statistics.

LULC Type	Area (ha)			
	1998		2020	
Vegetation	79993	27.6%	174	0.06%
Waterbody	24905	8.59%	2164	0.74%
Sand Dune	3130	1.08%	7992	2.75%
Bare Land	165187	57%	147636	51%
Cropland	15764	5.44%	119558	41.25%
Build Up	789	0.27%	1477	0.5%
Afforestation	-	-	10767	3.71%
Total	289768	100	289768	100

the total area in 1998 to 2.75% in 2020 and the build-up area shows growth from 0.27% of the total area in 1998 to 0.87% in 2020. In 2020LuLc map afforestation class is added with 10767 ha and occupied 3.71% of the total area of the watershed. Figure 4 presents comparative LULC classes graphically in the studied period.

Figure 4) Comparative change of LULC Classes area (ha) from 1998–2020.

Land-Use/ Land-Cover Change Rate and Pattern

Table 5 shows the cross-tabulation change matrix for the changed areas from one LULC class to another in comparison with

the total area of each LULC class from 1998 to 2020. During the study period, 93% of cropland remained unchanged, followed by bare land (71%), built-up (53%), water body (7%), sand dune (6%), and vegetation (0.05%). This indicates that vegetation experienced the most significant loss and highest conversion during this period, with almost 73% of its total area converted to cropland and bare land (22%) and the rest to other land-uses. The majority of the water body was converted to cropland (46%) and bare land (44%), while most of the bare land was converted to cropland (22%). The most important water source in the studied watershed was Sharifa Wetland, which is presented in the 98 LULC map (Figure 3), but unfortunately, agricultural and barren lands (Sabkha or saline land) replaced wetlands. Although a negligible area of water resources has been converted into build-up (0.05%), which seems to be related to the Persian Gulf freeway construction in Sharifa Wetland, it had a remarkable impact and western side lands have become barren due to the loss of hydrological connection [30].

Table 5) Transition matrix showing LULC change (ha) pattern.

ULC class	CL	WB	VE	BL	SD	BU
CL	**14715.26**	11632.36	58471.16	34525.21	93.23	206.14
WB	1.26	**1785.31**	226.09	123.55	2.8	0
VE	9.18	117.27	**43.04**	1.26	0	0
BL	653	11069.41	18201.3	**117315.55**	703.41	201.72
SD	29.65	28.35	588.16	4990.62	**205.38**	13.07
BU	90.5	13.87	247.86	632.71	7.6	422.76
AF	131.19	142.17	2445.6	7570.84	256.94	0

CL: Crop Land – WB: water body – VE: Vegetation – BL: Bare Land – SD: Sand dune – BU: Built Up
Note: The bold numbers on the diagonal represent unchanged LULC area (ha) from 1998 to 2020, while the others are the areas changed from one class to another.

Based on the change rate (Figure 5) cropland had the fastest growth rate close to 7, which means the area of croplands became 7 folds during the study period followed by sand dune (1.55) and build-up (0.87). Vegetation class experienced the fastest decline rate (-0.99) followed by water body (-0.9) and bare land (-0.1). The growth rate of sand dunes indicates an increase in wind erosion and loss of vegetation, due to degradation in the area.
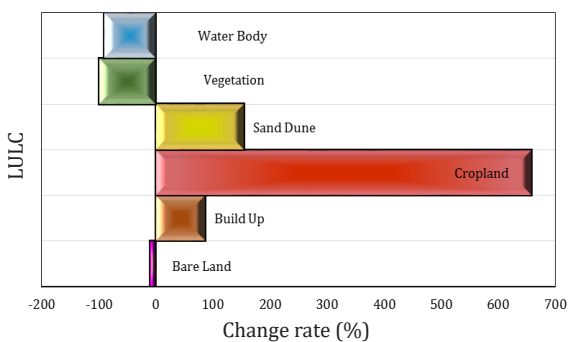

Figure 5) Change rate of LULC classes for 1998 and 2020.

Discussion

To answer the questions "How land-cover has changed over the past 22 years and what has been the main trend in LC change?" this research was conducted using remote sensing (RS) and geographic information systems (GIS). The maximum likelihood supervised classification technique was applied to Landsat images obtained for 1998 and 2020. Then, applying change detection on land-use maps and LC changes were extracted by a transition matrix. The findings showed that the model could simulate land-use classes in the study area with a kappa index accuracy of 0.85 and 0.86 respectively for 1998 and 2020. The pattern analysis of LC change over the past 22 years shows that the cropland, sand dune, and build-up area have increased at an average rate of approximately 658%, 155%, and 87% respectively; while vegetation cover, water body, and bare land have decreased by approximately 99%, 91% and 10%.

According to the findings, the decrease in vegetation cover and waterbodies was the consequence of the extension of cropland. Most of the cropland was occupied by vegetation cover and rangeland. This change of other LULC into cultivated land was supported by the change matrix tables. The results of the study in applying satellite images to detect land-cover changes in arid and semi-arid regions are in good agreement with Gheitury et al. [30]. Most changes happened between agriculture and rangeland

classes. Development of agriculture began at least two decades ago when the Government provided a new approach to agricultural products and raised economic growth based on increasing agricultural production [30]. This decline is linked not only to cropland expansion and development but also to free-ranging husbandry and overgrazing [30]. It also shows that, with population growth, the life of residents are still dependent on land (agriculture and husbandry) as the first source of life, due to underdevelopment, inadequate deterrence of laws, lack of accountability, transparency, and weakness of responsible institutions, uncontrolled human activities. This served as a major threat to the natural habitats and contributed significantly to the vegetation cover loss and environmental sustainability.

Conclusion

The study monitored and predicted the spatio-temporal LULC change in the Koupal Watershed in Khouzestan Province. Satellite data from different sensors and GIS techniques were employed to monitor the watershed LULC pattern using the land-cover maps of 1998 and 2020. In the study, the land-cover maps were classified into seven major LULC classes (built-up, vegetation, bare land, water bodies, sand dune, cropland, and afforestation). The results presented in this study showed significant changes in the spatial and quantitative distribution of LULC. It revealed the watershed's cropland area, built-up and sand dunes have grown continuously between 1998 and 2020, while bare land, water body, and vegetation decreased significantly during the study period. Such data are vital for informed decision-making in land planners, providing the potential information required to monitor growth and improve environmental sustainability.

Emphasis on development without considering sustainable development and socioeconomic problems lets beneficiaries be free in changing rangeland to agriculture.

Therefore, to balance the uncontrolled expansion of cropland and the preservation of the natural environment, policies that require rapid development without considering a balanced relationship between human activities and the environment need to be changed. This helps planners and other local managers effectively manage land-uses. It is essential to present some approaches to prevent further land-cover changes and land degradation. Initially, the economic problems of residents have to be solved to cut their dependence on land-based income, then increasing protection of national lands, intensifying fines for land-use change, and more importantly increasing the education on the negative impacts of LC changes. Further research needs to search more closely at the relationship between land-cover changes and population growth and socioeconomic conflicts.

Conflict of Interest

The author declares that there are no conflicts of interest regarding the publication of this manuscript.

data acquisition, M.D and K.B., and H.R.A All authors have read and agreed to the published version of the manuscript.

References

1. Halimi M., Sedighifar Z., Mohammadi C. Analyzing spatiotemporal land use/cover dynamic using remote sensing imagery and G.I.S techniques case: Kan Basin of Iran. GeoJournal. 2018;83(5): 1067-1077.

2. Twisa S., Buchroithner M. F. Land-use and land-cover (LULC) change detection in Wami River Basin, Tanzania. Land. 2019;8(9): 136-141.

3. Gifawesen S. T. Review on effects of land use land cover change on plant species composition, the case of Ethiopia. Bio. Agri. Healthcare. 2019;9(3): 40-51.

4. Mansour S., Al-Belushi M., Al-Awadhi T. Monitoring land use and land cover changes in the mountainous cities of Oman using G.I.S and Ca-Markov modelling techniques. Land Use Policy 2020;91(1): 80-95.

5. Koko A. F., Yue W., Abubakar G. A., Hamed R., Alabsi A. A. Monitoring and predicting spatio-temporal land use/land cover changes in Zaria city, Nigeria, through an Integrated Cellular Automata and Markov Chain model (CA-Markov). Land 2020;12(24): 104-128.

6. Naikoo M. W., Rihan M., Ishtiaque M., Shahfahad N. Analyses of land use land cover (LULC) change and built-up expansion in the suburb of a metropolitan city: Spatio-temporal analysis of Delhi using Landsat datasets. Urban Manag. 2020;9(3): 347-359.

7. Swain J. B., Patra K. C. Impact assessment of land use/land cover and climate change on streamflow regionalization in an ungauged catchment. Water Clim. Change 2018;10(3):554-568.

8. Traore M., Lee M. S., Rasul A., Balew A. Assessment of land use/land cover changes and their impacts on land surface temperature in Bangui (the capital of Central African Republic). Environ. Challenge. 2021;75(3):125-151.

9. Kamali Maskooni E., Hashemi H., Berndtsson R., Daneshkar Arasteh P., Kazemi M. Impact of spatiotemporal land-use and land-cover changes on surface urban heat islands in a semiarid region using Landsat data. Int. J. Digital Earth 2021;14(2):250-270.

10. Popov M., Michaelides S., Stankevich S., Kozlova A., Piestova I., Lubskiy M. Assessing long-term land cover changes in watershed by spatiotemporal fusion of classifications based on probability propagation: The case of Dniester River Basin. Remote Sens. Appl. Soc. Environ. 2021;25(4):90-135.

11. Chughtai A. H., Abbasi H., Karas I. R. A review on change detection method and accuracy assessment for land use land cover. Remote Sens. Appl: Soc. Environ. 2021;22(5): 112-137.

12. Si Salah H., Goldin S. E., Rezgui A., Nour El Islam B., Ait-Aoudia S. What is a remote sensing change detection technique? Towards a conceptual framework. Int. J. Remote Sens. 2020;41(5): 1788-1812.

13. Feranec J., Hazeu G., Christensen S., Jaffrain G. Corine land cover change detection in Europe (A case studies of the Netherlands and Slovakia). Land Use Policy 2007;24(1): 234-247.

14. Negassa M. D., Mallie D. T., Gemeda D. O. Forest cover change detection using geographic information systems and remote sensing techniques: A spatio-temporal study on Komto protected forest priority area, East Wollega Zone, Ethiopia. Environ. Syst. Res. 2020;9(1): 28-43.

15. Os B., Aa A. Change detection in land surface temperature and land use land cover over Lagos metropolis, Nigeria. J. O. R. S. G. 2016;5(3): 171-178.

16. Sam Navin M., Agilandeeswari L. Comprehensive review on land use/land cover change classification in remote sensing. J . Spectr. Imaging 2020;10(5): 200-215.

17. Hamidi M. Atmospheric investigation of frontal dust storms in southwest Asia. Asia-Pac. J. Atmos. Sci. 2018; 55(2): 177-193.

18. Campbell J. B., Wynne R. H. Introduction to remote sensing. The Guilford Press, 2011. 512 p.

19. Anonymous. Fundamentals of remote sensing. Canada Center for Remote Sensing, 2018. 450 p.

20. Richards J. S. Remote sensing digital image analysis. Springer, 2013. 502 p.

21. Jenson J. R. Introductory digital image processing: A remote sensing perspective, Pearson. 2015, 658 p.

22. Ikiel C., Dutucu A. A., Ustaoglu B., Kilic D. E. Land use and land cover (LULC) classification using spot-5 image in the Adapazari Plain and its surroundings, Turkey. T. O. J. S. A. T. 2012; 2(2): 37-43.

23. Tilahun A. Accuracy assessment of land use land cover classification using Google Earth. Am. J. Environ. Prot. Ecol. 2015;4(4):193-198.

24. Congalton R. G. Accuracy assessment and validation of remotely sensed and other spatial information. Int. J. Wildland Fire 2001;10(1) :321-328.

25. Janssen L.L.F., van der Wel F.J.M. Accuracy assessment of satellite derived land-cover data: A review. Photogram. Eng. Rem. S. 1994; 60 (4): 419-426.

26. Fung T., LeDrew E. The determination of optimal threshold levels for change detection using various accuracy indices. Photogram. Eng. Rem. S. 1988; 54 (10): 1449-1459.

27. Congalton R. G., Oderwald R. G., Mead R. A. Assessing Landsat classification accuracy using discrete multivariate analysis statistical techniques. Photogramm. Eng. Remote Sens.1983;9(12):1671-1678.

28. Lotfi Nasab S., Dargahian F., Khosrowshahi M. Water quality assessment of Koupal River and its variation in Maroon - Jarrahi Catchment. Water Eng. Manag. 2020; 12(3): 835-852. (In Persian)

29. Moradi F., Kaboli H. S., Lashkarara B. Projection of future land use/cover change in the Izeh-Pyon Plain of Iran using CA-Markov model. Arabian J. Geosci. 2020;13(19):997-1014.

30. Gheitury M., Heshmati M., Ahmadi M. Longterm land use change detection in Mahidasht Watershed, Iran. ECOPERSIA 2019;7(3): 141-148.

31. Khoshnood Motlagh S., Sadoddin A., Haghnegahdar A., Razavi S., Salmanmahiny A., Ghorbani K. Analysis and prediction of land cover changes using the land change modeler (lcm) in a semiarid river basin, Iran. Land Degrad. Dev. 2021;32(10): 3092-3105.